



This is a repository copy of *Absorption in ultrathin GaN-based membranes : the role of standing wave effects*.

White Rose Research Online URL for this paper:
<http://eprints.whiterose.ac.uk/151317/>

Version: Published Version

Article:

Amargianitakis, E.A., Jayaprakash, R., Kalaitzakis, F.G. et al. (3 more authors) (2019) Absorption in ultrathin GaN-based membranes : the role of standing wave effects. *Journal of Applied Physics*, 126 (8). ISSN 0021-8979

<https://doi.org/10.1063/1.5112173>

This article may be downloaded for personal use only. Any other use requires prior permission of the author and AIP Publishing. The following article appeared in *J. Appl. Phys.* 126, 083109 (2019); <https://doi.org/10.1063/1.5112173>.

Reuse

Items deposited in White Rose Research Online are protected by copyright, with all rights reserved unless indicated otherwise. They may be downloaded and/or printed for private study, or other acts as permitted by national copyright laws. The publisher or other rights holders may allow further reproduction and re-use of the full text version. This is indicated by the licence information on the White Rose Research Online record for the item.

Takedown

If you consider content in White Rose Research Online to be in breach of UK law, please notify us by emailing eprints@whiterose.ac.uk including the URL of the record and the reason for the withdrawal request.





eprints@whiterose.ac.uk
<https://eprints.whiterose.ac.uk/>

Absorption in ultrathin GaN-based membranes: The role of standing wave effects

Cite as: J. Appl. Phys. **126**, 083109 (2019); <https://doi.org/10.1063/1.5112173>

Submitted: 05 June 2019 . Accepted: 31 July 2019 . Published Online: 27 August 2019

E. A. Amargianitakis , R. Jayaprakash, F. G. Kalaitzakis, E. Delamadeleine, E. Monroy , and N. T. Pelekanos



View Online



Export Citation



CrossMark

ARTICLES YOU MAY BE INTERESTED IN

[Mechanisms of inhomogeneous broadening in InGaN dot-in-wire structures](#)

Journal of Applied Physics **126**, 083104 (2019); <https://doi.org/10.1063/1.5111343>

[Molecular beam epitaxy growth and optical properties of InAsSbBi](#)

Journal of Applied Physics **126**, 083101 (2019); <https://doi.org/10.1063/1.5098809>

[The role of Mg bulk hyper-doping and delta-doping in low-resistance GaN homojunction tunnel diodes with negative differential resistance](#)

Journal of Applied Physics **126**, 083110 (2019); <https://doi.org/10.1063/1.5112498>

Lock-in Amplifiers up to 600 MHz

starting at

\$6,210



 Zurich
Instruments

Watch the Video



Absorption in ultrathin GaN-based membranes: The role of standing wave effects

Cite as: J. Appl. Phys. 126, 083109 (2019); doi: 10.1063/1.5112173

Submitted: 5 June 2019 · Accepted: 31 July 2019 ·

Published Online: 27 August 2019



E. A. Amargianitakis,^{1,2,a)}  R. Jayaprakash,¹ F. G. Kalaitzakis,² E. Delamadeleine,³ E. Monroy,³ 
and N. T. Pelekanos^{1,2,a)}

AFFILIATIONS

¹Department of Materials Science and Technology, University of Crete, P.O. Box 2208, 71003 Heraklion, Greece

²Microelectronics Research Group, IESL-FORTH, P.O. Box 1385, 71110 Heraklion, Greece

³Université Grenoble-Alpes, CEA, INAC-PHELIQS, 17 av. des Martyrs, 38000 Grenoble, France

^{a)}Authors to whom correspondence should be addressed: amargian@materials.uoc.gr and pelekano@materials.uoc.gr

ABSTRACT

A methodology is described to extract the absorption coefficient spectrum and exciton oscillator strength of GaN layers and GaN/AlGaIn quantum wells by analyzing microtransmittance experiments in high-quality, free-standing membranes with thicknesses in the 160–230 nm range. The absorbance of a subwavelength GaN membrane is found to be an oscillating function of its thickness, in keeping with the standing wave effect. We analyze our results using two alternative models including interference effects and extract identical absorption coefficient values. The room-temperature absorption coefficient of bulk GaN membranes at the main exciton peak is found to be $9 \times 10^4 \text{ cm}^{-1}$. In the case of GaN/AlGaIn quantum wells, the enhancement and blue shift of the excitonic absorption are observed, as a result of quantum confinement.

Published under license by AIP Publishing. <https://doi.org/10.1063/1.5112173>

I. INTRODUCTION

After two decades of intensive research and technological development, gallium nitride (GaN) is now one of the major compound semiconductors with unique applications in violet/blue/green optoelectronics and in high-power electronics. In spite of the remarkable amount of information that is available in the literature on the optical and electronic properties of GaN, there are still several basic experiments that merit to be revisited based on newer developments in the field. For instance, the early measurements of absorption coefficient in GaN were performed on thin ($<1 \mu\text{m}$) GaN films, epitaxially grown on sapphire substrates,^{1–4} in order to maintain the transmittance signal above noise level. However, it is well known that such relatively thin GaN films on sapphire suffer from pronounced stacking disorder and high dislocation densities, owing to the 14.6% lattice mismatch between the two materials,⁵ which affect adversely their optoelectronic properties.⁶ In addition, these films present significant residual strain values of the order of 0.1%, altering the energy position and relative intensities of the A and B exciton lines.⁷ Similarly, due to opacity reasons of the GaN templates typically used for growth, there is a void in the literature of reliable absorption measurements on nitride alloys and heterostructures

around the energy gap of GaN, such as, for instance, GaN/AlGaIn quantum wells (QWs).

Lately, we have developed an alternative approach to fabricate high optical quality GaN membranes of subwavelength thickness with atomically smooth surfaces. The approach relies on the highly selective photoelectrochemical (PEC) etching of a thin InGaIn sacrificial layer,⁸ allowing for the detachment (in membrane form) of GaN-based films and heterostructures, which are coherently grown onto thick GaN/Al₂O₃ templates or bulk GaN substrates of superior crystalline quality. Using this PEC-etching technique, we have recently demonstrated ultrasoft GaN-based membranes with only 0.65 nm root-mean-square (rms) roughness of the etched N-face surface,⁹ as well as state-of-the-art membrane microcavities consisting of GaN/Al_{0.07}Ga_{0.93}N QWs sandwiched between dielectric distributed Bragg reflectors, which have shown room-temperature polariton lasing with the lowest quasicontinuous excitation threshold ever reported for a GaN bulk or QW polariton laser¹⁰ and a Rabi splitting as high as 71 meV.¹¹ Achieving similar results with alternative methods to fabricate GaN nanomembranes would not be a trivial task, considering, for instance, that in conductivity-selective electrochemical etching technique,^{12,13} the

rms roughness of the GaN etched surfaces remains considerably high, ~ 5 nm.¹⁴ Likewise, removing the substrate in GaN/Si¹⁵ and GaN/ZnO¹⁶ heterostructures by selective wet-etching would lead to relatively low quality GaN nanomembranes based on the defective heterogeneous growth of GaN on Si or ZnO. Accordingly, in this work, we employ the PEC etching approach and perform micro-transmittance (μ - T) experiments on high-quality free-standing GaN membranes with a varying thickness in the range from 160 to 230 nm. Considering the subwavelength thickness of the films, we develop a methodology taking into account the formation of standing waves inside the membranes, in order to turn the μ - T curves into actual absorption coefficient data. The method can be extended to any subwavelength structure. As an example, we deduce here the optical density and effective absorption coefficient of polar GaN/AlGaN QWs.

II. FABRICATION OF GaN-BASED MEMBRANES

The GaN-based membranes of this study are initially grown by plasma-assisted molecular beam epitaxy on commercial $8\ \mu\text{m}$ -thick n-type (0001)-oriented GaN/Al₂O₃ templates. For the fabrication of plain GaN membranes, the basic epitaxial structure consists of a GaN “active” layer with varying nominal thickness of 161, 194, and 226 nm, separated from the GaN/Al₂O₃ template by a 5 nm-thick In_{0.14}Ga_{0.86}N sacrificial layer. The 194 nm thickness corresponds to a $3\lambda_o/2n$ structure, with λ_o and n being the emission wavelength and refractive index at the gap of GaN, respectively. The other two thicknesses differ by $\pm\lambda_o/4n$ from the 194 nm thickness. For the study of GaN/AlGaN QWs, the basic epitaxial structure consists of 38 GaN/Al_{0.07}Ga_{0.93}N (2.7 nm/2.7 nm) QWs, separated from the GaN/Al₂O₃ template by a 25 nm-thick In_{0.14}Ga_{0.86}N sacrificial layer.

The as-grown samples are lithographically patterned into $1\ \mu\text{m}$ -deep square mesas with typical dimensions of $45 \times 45\ \mu\text{m}^2$ using reactive ion etching, to expose the lateral facets and enable selective PEC etching of the InGaN sacrificial layer^{8,9} [Fig. S1(a) in the [supplementary material](#)]. The PEC etching is performed in an electrochemical cell containing diluted KOH (4×10^{-4} M), under illumination by a few milliwatts of a continuous wave 405 nm diode laser for approximately 30 min. With this technique, we can achieve highly selective lateral etching of the InGaN layer and produce free-standing GaN membranes of high optical quality and subnanometer root-mean-square roughness.^{9,10} The free-standing GaN-based membranes are then transferred one by one, by taking advantage of attractive van der Waals interaction between a membrane and a probe tip, on $300\ \mu\text{m}$ -thick, double-side polished sapphire substrates for optical characterization [Fig. S1(a) in the [supplementary material](#)]. The μ - T spectra are recorded using a 0.5 m focal length, triple grating, imaging spectrograph, equipped with a liquid-nitrogen cooled charged coupled device detector. A normal incidence beam from a Xenon lamp is focused on the sample, and the transmitted signal is imaged with $\times 20$ magnification onto a $100\ \mu\text{m}$ diameter pinhole at the entrance of the spectrograph [Fig. S1(b) in the [supplementary material](#)]. To correct for the lamp’s spectral response, a transmission spectrum recorded next to each membrane is used as a reference. In [Figs. 1\(a\)–1\(c\)](#), we show top-view images of the GaN membranes of variable thickness

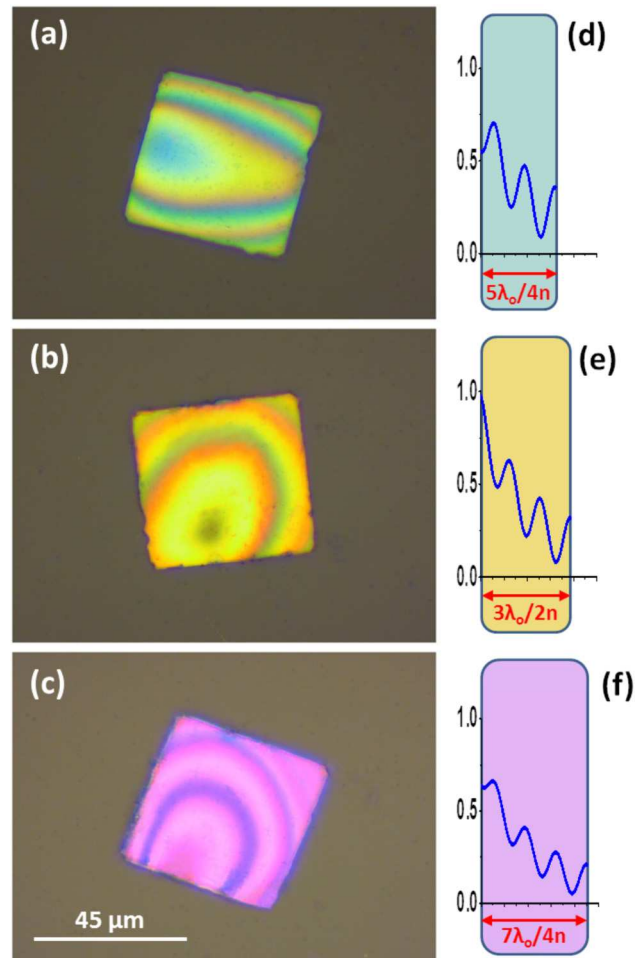


FIG. 1. Optical images of GaN membranes with thickness of (a) 163 nm, (b) 191 nm, and (c) 230 nm obtained in an optical microscope under front illumination. (d)–(f) Beam intensity profiles inside the GaN membranes, normalized to the intensity of the incident beam.

transferred on sapphire substrates. Their distinct color is directly associated to their thickness, as suggested by the reflectance simulations in Fig. S2 of the [supplementary material](#).

III. RESULTS AND DISCUSSION

For each membrane, its thickness is precisely determined by fitting the Fabry-Perot oscillations in the transparent part of the μ - T spectra, as presented in [Fig. 2](#). The theoretical curves are based on a transfer-matrix model assuming a free-standing nonabsorbing GaN layer and are very sensitive to the GaN thickness, which is the only adjustable parameter. The GaN refractive index below the bandgap is taken from the data of Kazazis *et al.*¹⁷ For simplicity, the refractive index is assumed to remain constant above the bandgap. The membrane is considered as free-standing based on

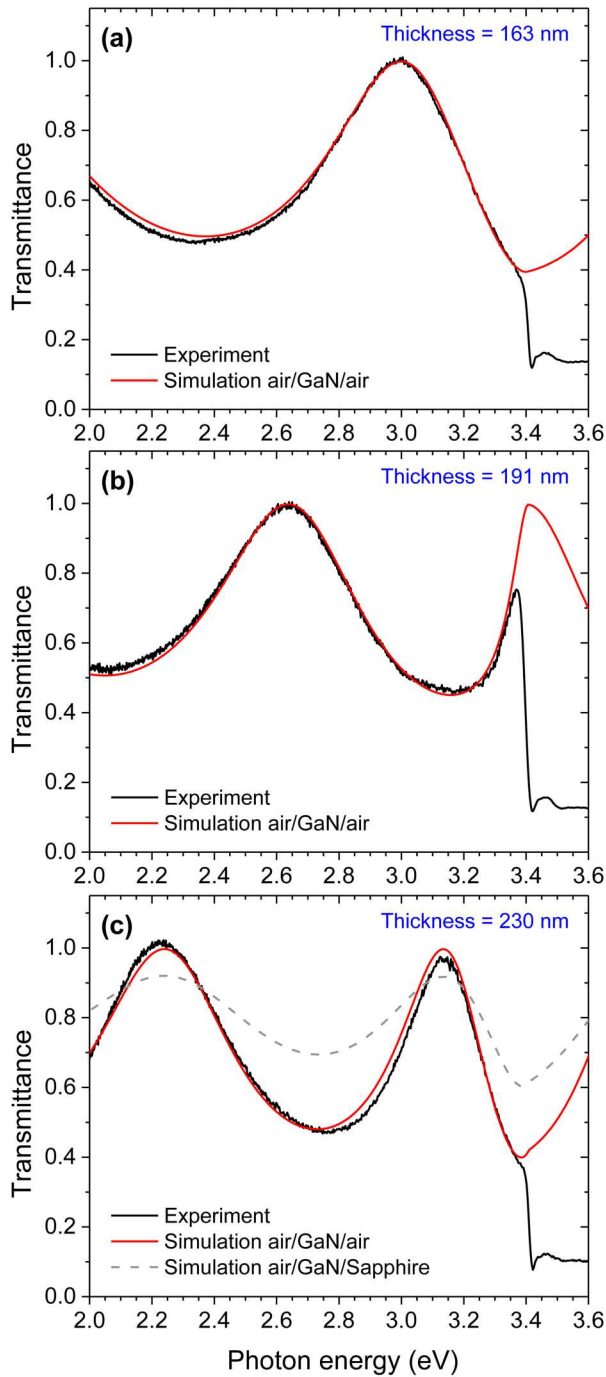


FIG. 2. Micro-transmittance spectra obtained at room temperature from GaN membranes with thicknesses (a) 163 nm, (b) 191 nm, and (c) 230 nm, as determined by fitting the transparent part of the spectra based on a transfer matrix model neglecting absorption, assuming an air/GaN/air configuration and using the GaN thickness as the sole adjustable parameter. The dashed curve in (c), corresponding to an air/GaN/sapphire configuration, fails to reproduce the experimental curve.

the excellent fit of the transparent region of the μ - T spectra obtained under the assumption of an air/GaN/air structure. This is illustrated in Fig. 2(c), where we observe that the simulated air/GaN/sapphire curve fails to reproduce the “depth” of the Fabry-Perot oscillations, unlike the air/GaN/air configuration that provides an excellent fit. Further evidence that the GaN membranes are actually free-standing is provided by scanning electron microscopy images of GaN membranes transferred to sapphire (e.g., see Fig. S3 in the supplementary material), where it is clear that the GaN membrane is kept at a distance from the substrate due to processing-related residues preventing a close contact.

Aside from the excellent agreement between simulated and experimental curves for energies below the bandgap energy, all μ - T spectra in Fig. 2 present a pronounced GaN excitonic absorption dip, centered precisely at 3.422 eV. A zoom-in of the μ - T spectrum around the GaN bandgap is given in Fig. S4 of the supplementary material for one of the samples. The dip corresponds to a merged A + B exciton absorption peak, and its energy position is in good agreement with the A and B exciton energies reported in unstrained homoepitaxial GaN thin films¹⁸ and in fully relaxed GaN nanowires.¹⁹

Considering the subwavelength ($d < \lambda$) thickness of the membranes, it is necessary to include the standing wave effect in our analysis. Toward this end, a first approach is solving a three-layer Fabry-Perot structure of the type “medium 1/GaN/medium 2” of thickness d under normal incidence. Using a transfer matrix model, the expressions for the transmittance (T) and reflectance (R)²⁰ are as follows:

$$T(\lambda, d) = \frac{(1 - R_1)(1 - R_2)e^{-ad}}{(1 - R''e^{-ad})^2 + 4R''e^{-ad}\sin^2(\beta d)}, \quad (1)$$

$$R(\lambda, d) = \frac{(\sqrt{R_1} - \sqrt{R_2}e^{-ad})^2 + 4R''e^{-ad}\sin^2(\beta d)}{(1 - R''e^{-ad})^2 + 4R''e^{-ad}\sin^2(\beta d)}, \quad (2)$$

where a is the absorption coefficient of GaN at wavelength λ , $R_1(\lambda)$ and $R_2(\lambda)$ are the power reflectivities at the interfaces of GaN with medium 1 and 2, respectively, $R'' = \sqrt{R_1 R_2}$, and $\beta = 2\pi \text{Re}(n)/\lambda$. In Fig. 3(a), we plot for a symmetric air/GaN/air structure the calculated transmittance curves obtained at the A + B exciton position of 3.422 eV as a function of GaN thickness and for various values of the absorption coefficient. All T -curves exhibit the characteristic oscillatory behavior due to the standing wave effect, while the T -curve that reproduces best the experimental values measured on several membranes is the one corresponding to an absorption coefficient at the A + B exciton peak of $a = 9 \times 10^4 \text{ cm}^{-1}$. This value is in good agreement with previous reports on the absorption coefficient of GaN.^{3,4} From Eq. (1), the optical density, $OD = a \times d$, can be readily approximated as follows:

$$OD(\lambda, d) \approx \ln \left[\frac{(1 - R_1)(1 - R_2)}{T(\lambda, d)} - 4R''\sin^2(\beta d) + 2R'' \right]. \quad (3)$$

Introducing in Eq. (3), the experimental $T(E = 3.422 \text{ eV}, d)$ values and the respective refractive index of GaN,¹⁷ we obtain in Fig. 3(b) the expected linear dependence of the optical density at

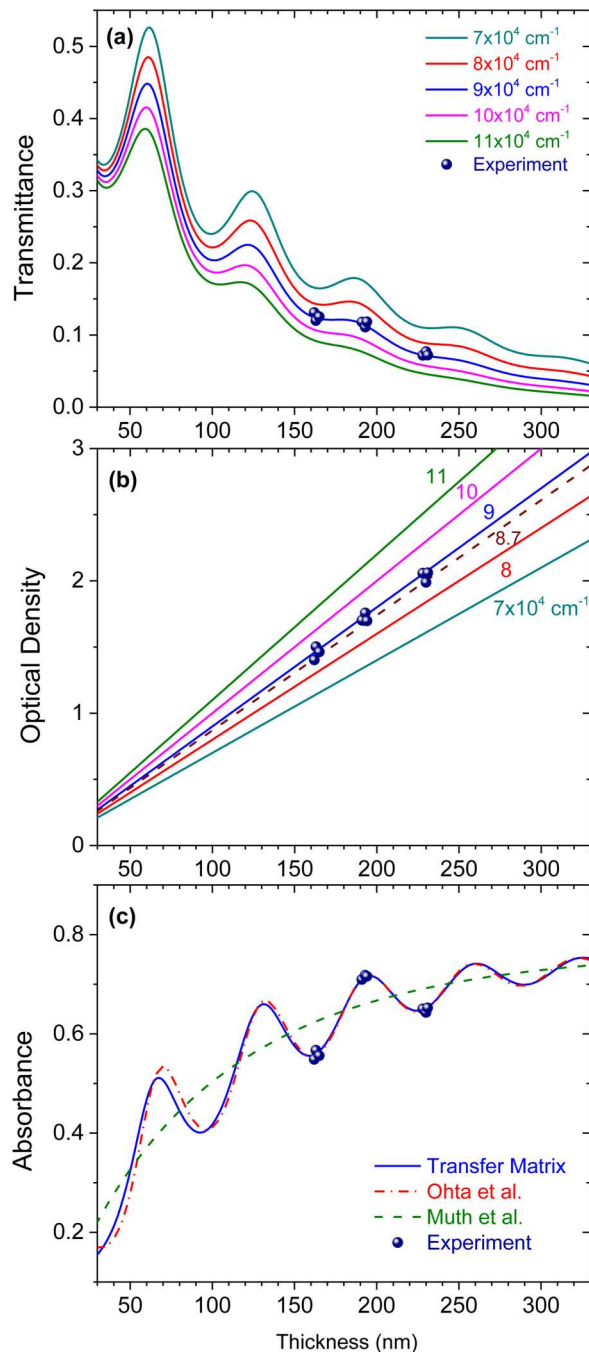


FIG. 3. (a) Simulated transmittance at the A + B exciton position of GaN as a function of membrane thickness, estimated for various absorption coefficient values. (b) Optical density of the fabricated GaN membranes vs thickness and comparison with linear curves corresponding to different absorption coefficient values. (c) Experimental absorbance compared to theoretical absorbance curves obtained using $a = 9 \times 10^4 \text{ cm}^{-1}$ in the transfer matrix model equations, the model proposed by Ohta and Ishida,^{21,22} and the model used by Muth *et al.*⁴

the given energy on the film thickness, with the experimental points following closely the line with slope $a = 9 \times 10^4 \text{ cm}^{-1}$. On the other hand, if we introduce in Eq. (3) the $T(E)$ spectra for a given d and the dispersion of the GaN refractive index, we can extract the OD spectrum for the given thickness (cf. Fig. S6 in the [supplementary material](#)), and thereby the absorption coefficient of the GaN membrane, as shown in Fig. 4 for the 163 nm-thick GaN membrane (solid curve).

Next, we deduce for each membrane the absorbance ($A = 1 - T - R$) at the A + B exciton position, by estimating R through Eq. (2), using $a = 9 \times 10^4 \text{ cm}^{-1}$. In Fig. 3(c), we compare the experimental values of absorbance with various theoretical models. Excellent agreement is observed with those models that take into account interference effects, such as the transfer matrix model discussed above (solid curve) and an alternative approach proposed by Ohta and Ishida²¹ (dot-dashed curve). In the latter model, the absorbance A is calculated using Poynting's theorem and is related to the normalized beam intensity profile $I(z)$ inside the film, according to

$$A = \int_0^d a(z)I(z)dz. \quad (4)$$

For a homogeneous film, a is constant and A becomes proportional to the absorption coefficient and to the integral of $I(z)$ inside the film. The normalized intensity profiles can be estimated as a function of film thickness following Ref. 22. As an example, we plot in Figs. 1(d)–1(f) the intensity profiles for the three types of GaN membranes used in this work. For comparison purposes, these profiles are represented on the same graph in Fig. S5 of the [supplementary material](#). It is important to note that the integral of the $3\lambda_o/2n$ -profile is larger than the integrals of the $5\lambda_o/4n$ - and $7\lambda_o/4n$ -profiles, accounting for the higher absorbance of

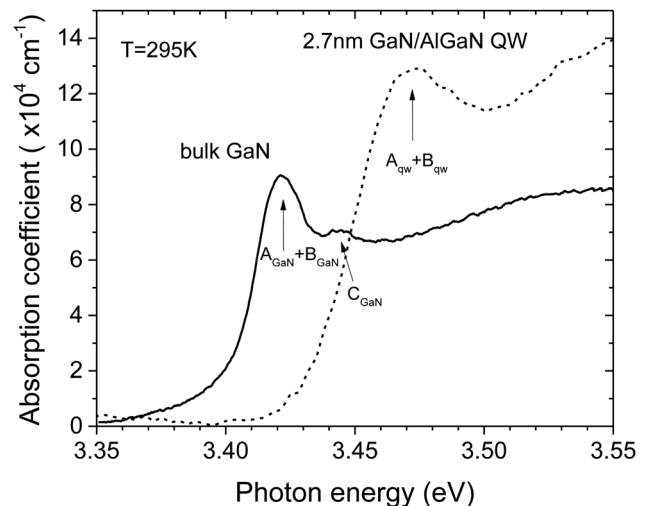


FIG. 4. Absorption coefficient spectra of bulk GaN (solid) and of GaN/Al_{0.07}Ga_{0.93}N QWs with 2.7 nm well and barrier thicknesses (dashed), deduced from measurements on ultrathin membranes. The various excitonic transitions in the respective samples are indicated by arrows.

the $3\lambda_c/2n$ -thick membranes. Finally, the dashed curve in Fig. 3(c), obtained considering multiple reflections but ignoring interference,⁴ clearly fails to reproduce the experimental results, illustrating, thus, the crucial role of the standing wave effect in our structures.

The above-described analysis can be easily extended to GaN/AlGaIn QWs, with some minor modifications. The starting point is to determine, along with the membrane thickness, an effective refractive index $n_{\text{eff}}(\lambda)$ for the GaN/AlGaIn heterostructure. This is achieved by fitting the low-energy Fabry-Perot oscillations of the μ - T spectrum using Eq. (1) and assuming a spectral dependence of $n_{\text{eff}}(\lambda)$ similar to AlGaIn.²³ Next, by inserting the experimental transmittance data and fitted parameters in Eq. (3), we can derive the optical density spectrum $OD(E)$ of the entire membrane (cf. Fig. S6 in the supplementary material). In a QW-containing membrane, the optical density can be written as $OD(E) = N_{\text{qw}} \times L_{\text{qw}} \times \alpha_{\text{qw}}(E)$, where N_{qw} is the number of QWs, L_{qw} is the well thickness, and $\alpha_{\text{qw}}(E)$ is the effective absorption coefficient of the QW material. The resulting absorption coefficient spectrum of the GaN/Al_{0.07}Ga_{0.93}N (2.7 nm/2.7 nm) QWs under study is plotted as dashed curve in Fig. 4. The spectrum shows a pronounced excitonic peak around 3.47 eV, corresponding to a merged “A + B” QW exciton peak, which is considerably blue-shifted and enhanced compared to the bulk case due to quantum confinement.

We estimate next the oscillator strength per unit area and per QW of the “A + B” QW exciton using the relation^{24,25}

$$\frac{f_{\text{qw}}}{S} = \frac{2\epsilon_0 n_{\text{eff}} m_0 c}{\pi e^2 \hbar} \times \frac{\int OD(E) dE}{N_{\text{qw}}}. \quad (5)$$

The optical density integral is estimated by fitting the “A + B” QW exciton line in Fig. S6 of the supplementary material with two Gaussians, corresponding to the A and B QW excitons, distanced by 10 meV. The resulting value for the “A + B” QW exciton oscillator strength per unit area and per QW of the 2.7 nm GaN/AlGaIn QW is found to be $4.5 \times 10^{13} \text{ cm}^{-2}$, in good agreement with previous reports for similar QWs that were based on polariton dispersion analysis.²⁶ Finally, following a similar analysis for the bulk GaN described in supplementary information, we also obtain the oscillator strength per unit volume for the GaN A + B exciton line, $f_{\text{GaN}}/V = 8.5 \times 10^{19} \text{ cm}^{-3}$.

IV. CONCLUSION

In summary, we establish here a new approach for measuring absorption coefficients and exciton oscillator strengths in nitride films and heterostructures, circumventing possible substrate-related limitations such as low quality or opacity. The method relies on transmittance measurements on ultrasmooth GaN-based membranes, which are detached following a highly selective lateral etching step. Interference effects, which are crucial in these sub-wavelength structures, are explicitly taken into account. We deduce here as examples the absorption coefficient spectra and oscillator strength of polar GaN films and GaN/AlGaIn quantum wells.

SUPPLEMENTARY MATERIAL

See the supplementary material for experimental schematics and further details on the absorption analysis of GaN-based membranes.

ACKNOWLEDGMENTS

E.A.A. is supported by the Hellenic Foundation for Research and Innovation (HFRI) and the General Secretariat for Research and Technology (GSRT) under the HFRI Ph.D. fellowship grant (GA. No. 195). This work is supported in part by the European Research Infrastructure NFFA-Europe, funded by EU's H2020 framework program for research and innovation under Grant Agreement No. 654360.

REFERENCES

- 1 H. Amano, N. Watanabe, N. Koide, and I. Akasaki, *Jpn. J. Appl. Phys.* **32**, L1000 (1993).
- 2 M. O. Manasreh, *Phys. Rev. B* **53**, 16425 (1996).
- 3 A. J. Fischer, W. Shan, J. J. Song, Y. C. Chang, R. Horning, and B. Goldenberg, *Appl. Phys. Lett.* **71**, 1981 (1997).
- 4 J. F. Muth, J. H. Lee, I. K. Shmagin, R. M. Kolbas, H. C. Casey, Jr., B. P. Keller, U. K. Mishra, and S. P. DenBaars, *Appl. Phys. Lett.* **71**, 2572 (1997).
- 5 X. H. Wu, L. M. Brown, D. Kapolnek, S. Keller, B. Keller, S. P. DenBaars, and J. S. Speck, *J. Appl. Phys.* **80**, 3228 (1996).
- 6 S. Nakamura, *Science* **281**, 956 (1998).
- 7 A. Shikanai, T. Azuhata, T. Sota, S. Chichibu, A. Kuramata, K. Horino, and S. Nakamura, *J. Appl. Phys.* **81**, 417 (1997).
- 8 E. Trichas, M. Kayambaki, E. Iliopoulos, N. T. Pelekanos, and P. G. Savvidis, *Appl. Phys. Lett.* **94**, 173505 (2009).
- 9 R. Jayaprakash, F. G. Kalaitzakis, M. Kayambaki, K. Tsagaraki, E. Monroy, and N. T. Pelekanos, *J. Mater. Sci.* **49**, 4018 (2014).
- 10 R. Jayaprakash, F. G. Kalaitzakis, G. Christmann, K. Tsagaraki, M. Hocevar, B. Gayral, E. Monroy, and N. T. Pelekanos, *Sci. Rep.* **7**, 5542 (2017).
- 11 E. A. Amargianitakis, F. Miziou, M. Androulidaki, K. Tsagaraki, A. Kostopoulos, G. Konstantinidis, E. Delamadeleine, E. Monroy, and N. T. Pelekanos, *Phys. Status Solidi B* **256**, 1800716 (2019).
- 12 S. H. Park, G. Yuan, D. Chen, K. Xiong, J. Song, B. Leung, and J. Han, *Nano Lett.* **14**, 4293–4298 (2014).
- 13 K. Xiong, S. H. Park, J. Song, G. Yuan, D. Chen, B. Leung, and J. Han, *Adv. Funct. Mater.* **24**, 6503–6508 (2014).
- 14 D. Chen and J. Han, *Appl. Phys. Lett.* **101**, 221104 (2012).
- 15 Y. Mei, D. J. Thurmer, C. Deneke, S. Kiravittaya, Y.-F. Chen, A. Dadgar, F. Bertram, B. Bastek, A. Krost, J. Christen, T. Reindl, M. Stoffel, E. Coric, and O. G. Schmidt, *ACS Nano* **3**, 1663–1668 (2009).
- 16 J. Wang, E. Song, C. Yang, L. Zheng, and Y. Mei, *Thin Solid Films* **627**, 77–81 (2017).
- 17 S. A. Kazazis, E. Papadomanolaki, M. Androulidaki, M. Kayambaki, and E. Iliopoulos, *J. Appl. Phys.* **123**, 125101 (2018).
- 18 K. Kornitzer, T. Ebner, K. Thonke, R. Sauer, C. Kirchner, V. Schwegler, M. Kamp, M. Leszczynski, I. Grzegory, and S. Porowski, *Phys. Rev. B* **60**, 1471 (1999).
- 19 R. Jayaprakash, D. Ajagunna, S. Germanis, M. Androulidaki, K. Tsagaraki, A. Georgakilas, and N. T. Pelekanos, *Opt. Express* **22**, 19555 (2014).
- 20 L. A. Coldren and S. W. Corzine, *Diode Lasers and Photonic Integrated Circuits* (Wiley-Interscience, 1995).
- 21 K. Ohta and H. Ishida, *Appl. Opt.* **29**, 2466 (1990).
- 22 K. Ohta and H. Ishida, *Appl. Opt.* **29**, 1952 (1990).
- 23 G. M. Laws, E. C. Larkins, I. Harrison, C. Molloy, and D. Somerford, *J. Appl. Phys.* **89**, 1108 (2001).
- 24 Y. Masumoto, M. Matsuura, S. Tarucha, and H. Okamoto, *Phys. Rev. B* **32**, 4275 (1985).
- 25 Y. Yamamoto, F. Tassone, and H. Cao, *Semiconductor Cavity Quantum Electrodynamics* (Springer, 2010).
- 26 G. Christmann, R. Butté, E. Feltn, A. Mouti, P. A. Stadelmann, A. Castiglia, J.-F. Carlin, and N. Grandjean, *Phys. Rev. B* **77**, 085310 (2008).